

# UNCERTAINTIES IN THE ANALYSIS OF AVOA FOR DETERMINATION OF FRACTURE ORIENTATION

## S. HARWOOD

Elf Geoscience Research Center<sup>1</sup>  
Leeds University<sup>2</sup>  
Now Queen's University, Canada<sup>3</sup>

## P. S. ROWBOTHAM, I. BUSH and P. R. WILLIAMSON

Elf Geoscience Research Centre<sup>1</sup>

## H. HOULLEVIGUE

Elf Exploration Production<sup>4</sup>

## J. M. KENDALL

Leeds University<sup>2</sup>

## INCERTITUDES DANS L'ANALYSE DE L'AVOA UTILISÉE POUR DÉTERMINER L'ORIENTATION DES FRACTURES

La variation d'amplitude de réflexion d'une onde P avec l'offset et l'azimut (AVOA) indique une anisotropie azimutale dans au moins une des couches entourant le réflecteur. La cause vraisemblable d'une telle anisotropie est la présence d'un ensemble de fissures ou de fractures alignées verticalement. Nous présentons ici l'étude AVOA d'un cas concret sur un jeu de données sismiques marines multi-azimutales en 3D. Nous considérons deux approches pour évaluer l'orientation d'un ensemble de fractures hypothétiques et tentons d'estimer les incertitudes des paramètres concernés. Ceci nous permet d'identifier quelles variations d'amplitude sont significatives. Certaines tendances locales sont visibles, mais il ne semble pas y avoir globalement d'orientation préférentielle. Malheureusement, les résultats de notre analyse ne peuvent pas être confirmés en raison de l'absence d'autres données (par exemple, de puits).

## UNCERTAINTIES IN THE ANALYSIS OF AVOA FOR DETERMINATION OF FRACTURE ORIENTATION

Amplitude variation with offset and azimuth (AVOA) of a P-wave reflection indicates azimuthal anisotropy in at least one of the layers surrounding the reflector. A likely cause of such anisotropy is a set of aligned vertical cracks or fractures. We present a case study of AVOA analysis of a single reflection in a portion of a 3-D multi-azimuthal seismic marine dataset. We consider two approaches to estimating the orientation of a hypothetical fracture set and attempt to assess the uncertainties in the relevant parameters. This allows us to identify which amplitude variations are significant. Some local trends can be seen, but there does not appear to be any globally-preferred orientation. Unfortunately the results of our analysis cannot be confirmed due to the absence of other data (e.g. from wells).

## INCERTIDUMBRES RESPECTO AL ANÁLISIS DE LA AVOA PARA DETERMINAR LA ORIENTACIÓN DE FRACTURAS

La variación de la amplitud con compensación y azimut (AVOA) del reflejo de una onda P indica anisotropía azimutal de por lo menos una de las capas que rodean el reflector. Una causa probable de dicha anisotropía es un conjunto de grietas o fracturas verticales alineadas. Presentamos un estudio de caso de análisis

(1) 30 Buckingham Gate,  
London SW1E 6NN - United Kingdom

(2) Department of Earth Sciences,  
University of Leeds,  
Leeds LS2 9JT - United Kingdom

(3) Department of Geological Sciences,  
Kingston, Ontario - Canada K7L 3N6

(4) Centre scientifique et technique Jean Feger,  
Avenue Larribau,  
64018 Pau - France

mediante AVOA para una única reflexión en una porción de un conjunto de datos marinos sísmicos multiazimutales tridimensionales. Consideramos dos enfoques para estimar la orientación de un conjunto hipotético de fracturas e intentar una evaluación de las incertidumbres en los parámetros relevantes. Esto nos permite identificar qué variaciones de amplitud son significativas. Pueden observarse algunas tendencias locales, pero no parece haber ninguna orientación globalmente preferente. Desgraciadamente, los resultados de nuestro análisis no pueden ser confirmados debido a la ausencia de otros datos (p. ej., de pozos).

## INTRODUCTION

Cracks and fractures may be significant sources of porosity and permeability in hydrocarbon reservoirs. When aligned they will typically define local preferred flow directions, so information as to the orientation of sets of fractures or cracks may be useful in reservoir management. This information may be inferred from the consequent azimuthal elastic anisotropy: seismic signatures include shear-wave birefringence (Crampin, 1984), azimuthal dependence of seismic velocities (Lynn *et al.*, 1995) and AVOA for reflections from top and bottom of the fractured layer (Mallick *et al.*, 1996).

We here perform *P*-wave AVOA analysis of a reflection over an area of approximately 1 km by 1 km taken from a 3D marine dataset in which data were recorded for four sail directions at 45° azimuthal increments. The reflector is at the top of a layer interpreted as being more brittle than the surrounding ones and there have been significant local salt flows below this layer which may have caused fracturing within the layer.

We initially used the method of Mallick *et al.* (1996), in which the amplitude variation with azimuth at constant offset is studied. A second approach inverts all the data in a CMP bin by using a Shuey (1985) type model of reflection amplitudes which includes offset dependence, i.e., a true AVOA analysis. Both models assume elliptical azimuthal variation, which is valid when the offsets are not too large (Corrigan, 1990). The second method is more stable against the effects of noise and allows for irregular acquisition geometry (especially important for near offsets). It also allows more convenient analysis of the uncertainties in the results, e.g. using the posterior covariance matrix, and therefore an assessment of which, if any, are the significant trends in our results. This is of vital importance if AVOA is to be promoted as a prediction tool for well planning.

## METHOD

### Pre-Analysis Processing

The data from all four sail directions were initially binned into a common 28 x 28 m grid. The main steps of the processing sequence were velocity analysis, correction for geometrical spreading, NMO, and

amplitude picking. Velocity analysis was performed for one sail direction only—subsequent NMO correction of all the data revealed negligible residual moveout for all azimuths, suggesting that there was little *P*-wave azimuthal anisotropy above the target reflector. Variation of velocity with position was also small and smooth. Due to the relative strength of the reflection locally, the amplitude was picked as the maximum over an 11 sample (33 ms) window, using sinc interpolation. The data going forward from the processing were therefore the bin coordinates (CMP and line number), azimuth, offset (and estimated incidence angle), and the picked amplitude. One concern was the possibility that there might be differences in amplitude due to acquisition effects for the four different sail directions. This was checked by performing standard AVO analysis for each direction and comparing the estimated zero-offset reflectivities, which were consistent for all directions.

**Azimuthal Amplitude Analysis**

We have applied two amplitude analysis methods to the picked data. The first, based on Mallick *et al.* (1996), looks at the azimuthal variation of amplitude in constant-offset gathers. The second inverts all the data in each CMP bin at once for the “generalised Shuey” parameters describing the limited offset approximate AVOA. For both methods, we assume that any azimuthal anisotropy in the data may be approximated by elliptical variation, as might arise from a set of aligned fractures in an otherwise homogenous porous isotropic rock (Thomsen, 1995).

**Method 1: Rose fracture plots**

The method of Mallick *et al.* (1996) uses the fact that for a given (not too large) offset, the amplitude of a *P*-wave reflection *v* from a horizontal interface may vary with azimuth approximately as:

$$v = A + B \cos 2(\phi - \phi_0) \tag{1}$$

where:

- *A* is an offset-dependent bias;
- *B* is an offset-dependent amplitude modulation factor related to the change in anisotropy across the interface (thus containing information about possible fracture properties);
- $\phi$  is the azimuth;

- $\phi_0$  is the azimuth origin corresponding to a vertical symmetry plane (e.g., fracture strike).

With amplitude data from three or more azimuths *A*, *B* and  $\phi_0$  may be recovered.  $\phi_0$  was estimated for each offset independently, and from all possible triplet combinations at that offset from the available azimuths at each bin location. The results from each bin are plotted as an angular histogram (rose plot) at the corresponding location. Figure 1 shows results with each triplet of amplitudes being weighted by the factor *B/A* in the rose plots. Those triplets with strong azimuthal amplitude variation have a large value of *B* relative to *A*, and will therefore be weighted more strongly. A moving two-by-two bin averaging window across the bins has been applied to reduce scatter. The empty portions of the plot correspond to areas where data from at least one sail direction is missing or of poor data quality. Some directional trends are discernible in this figure, such as one at about 60° in the location around line 1783, CMP 290, although there is no one global trend within the data.

Sub-dividing these rose-plots in terms of offset ranges provides evidence that some bins have conflicting contributions from near and far offsets.

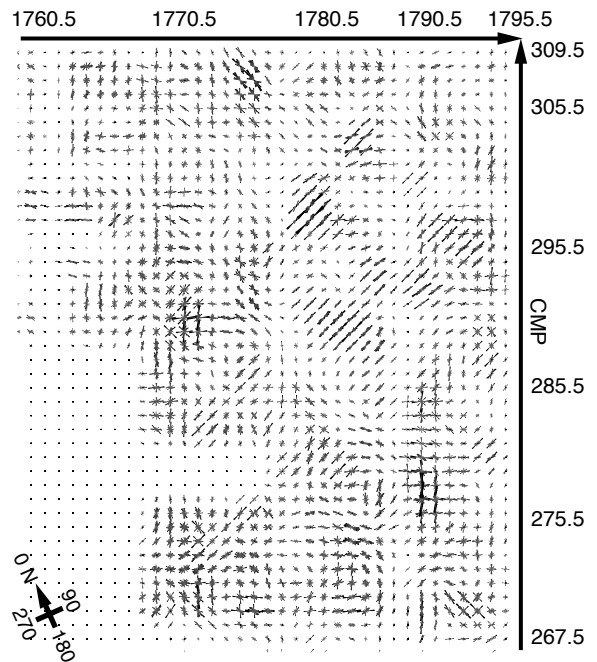


Figure 1

Rose plot.

Despite the appeal of the simplicity of this method, we have therefore moved to Method 2 which accounts for amplitude variations across offsets.

**Method 2: AVOA inversion by bin**

To lowest order (i.e. for short-moderate offset ranges) the amplitude picks can be modelled by an “extension” of the Shuey equation to include azimuthal variation:

$$v(\theta, \phi) = R_0 + \sin^2 \theta (G + B \cos 2(\phi - \phi_0)) \quad (2)$$

where:

- $\theta$  is the incidence angle;
- $R_0$  and  $G$  are generalisations of the Shuey intercept and gradient parameters;
- $B$  is the magnitude of the azimuthal variation of  $G$ ;
- $\phi$  and  $\phi_0$  are as before.

The relations of these parameters to the elastic properties of the media on either side of the reflector have been given for the special case of HTI by Rüger (1996). Figure 2 shows the behaviour of this modelled amplitude as a function of incidence and azimuth angles.

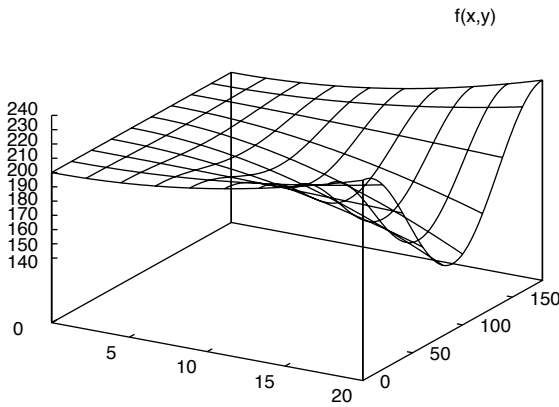


Figure 2  
AVOA surface.

We can expect greater accuracy and stability of parameter estimation by inverting this equation using all the data in a given CMP bin than by the offset-by-offset approach of Method 1. This may be achieved by minimising the L2 norm objective function,  $D$ :

$$D = \sum_{i=1}^n [v(\theta_i, \phi_i) - A_i]^2 \quad (3)$$

where:

- $A_i$  are the amplitude picks;
- $v$  are the modelled amplitudes for the corresponding azimuths and incidence angles;
- $n$  is the number of amplitude picks in the bin.

Initial results looked “noisy” so we further stabilised the inversion by including all data from three-by-three bins to estimate the parameters of the central one. We note that the dimensions of this “superbin” (85 m square) are comparable to the radius of the first Fresnel zone at the reflector, and thus the smoothing is partially justified on physical grounds. Results of the inversion are shown in Figures 3-7.

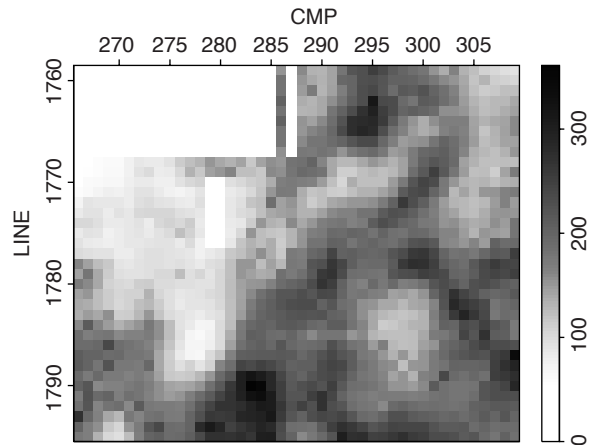


Figure 3  
L2-norm intercept ( $R_0$ ).

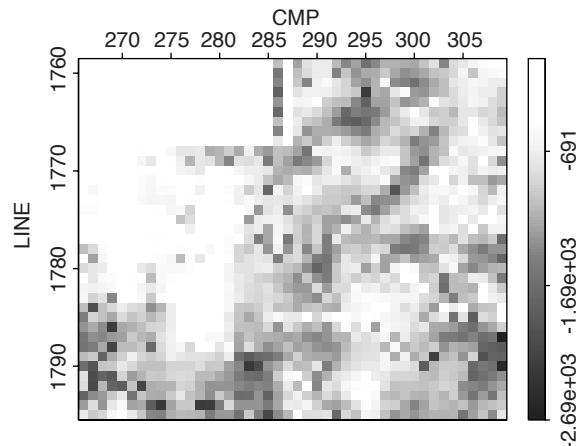


Figure 4  
L2-norm gradient ( $G$ ).

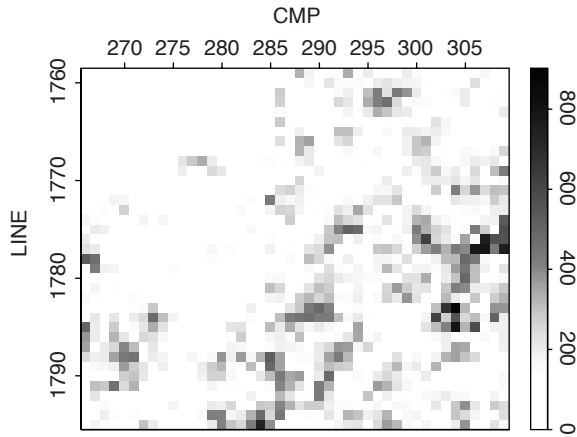


Figure 5  
L2-norm  $B$ .

Because there is no interpretable global trend in the recovered values of  $\phi_0$ , and the values of the other parameters fluctuate quite strongly, we repeated the inversion as an L1 optimisation, so as to check for the influence of outliers/non-Gaussian noise on the original inversion. However, the differences from the L2 results are so small that we saw no benefit in abandoning the convenience of the L2 formalism for subsequent analysis. The values of  $B$  are in general small compared to  $G$ , provoking some doubt as to whether the estimated azimuthal variation was real or merely fitting noise. In an initial attempt to address this question we first repeated the inversion with  $B$  held to be zero, i.e., we

inverted for  $R_0$  and  $G$  only. The resultant parameters were almost identical to those from the full inversion, and the level of data residuals was not much greater. However, we can attempt to assess the significance of these differences by considering the posterior model covariance matrix  $C_m$ . This matrix can straightforwardly be constructed assuming that the (approximate) RMS value of the data residuals from the initial inversion is a good estimate of the noise standard deviation (we use an approximate RMS with the denominator as  $(n-4)$  rather than  $n$  since there are four model parameters). Also it is assumed that the residuals are mutually independent and that the modelled amplitudes are approximately linear functions of the parameters at the solution. Then we have:

$$C_m = \sigma_a^2 (G^T G)^{-1} \quad (4)$$

where  $\sigma_a$  is the estimate of the noise level of the picked amplitudes, and:

$$G_{ij} = \frac{\partial v_i}{\partial m_j} \quad (5)$$

where  $m_j$  denotes one of the model parameters.

Figures 8-10 show estimated deviations for the parameters  $G$ ,  $B$  and  $\phi_0$ , and Figures 11 and 12 the deviation of  $G$  and  $B$  normalised by the respective parameter values. The estimated deviations for  $\phi_0$  are generally small ( $< 5^\circ$ ), so in regions where the normalised deviation of  $B$  is appreciably less than one, the angular trends shown in Figures 6 and 7 can be

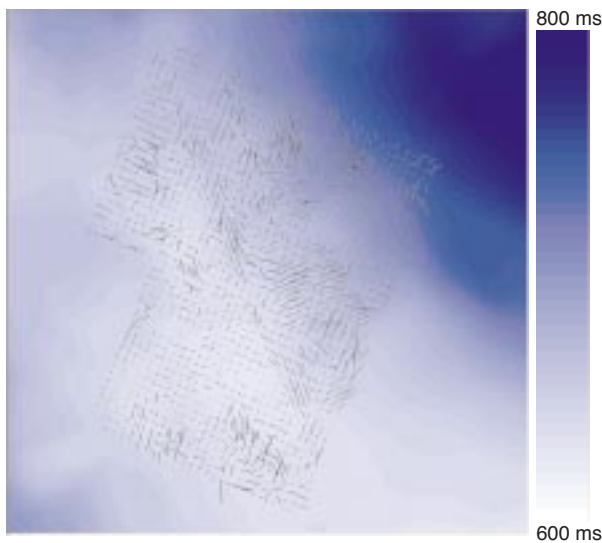


Figure 6  
 $\phi_0$  weighted by  $B$  on top of the picked time horizon.

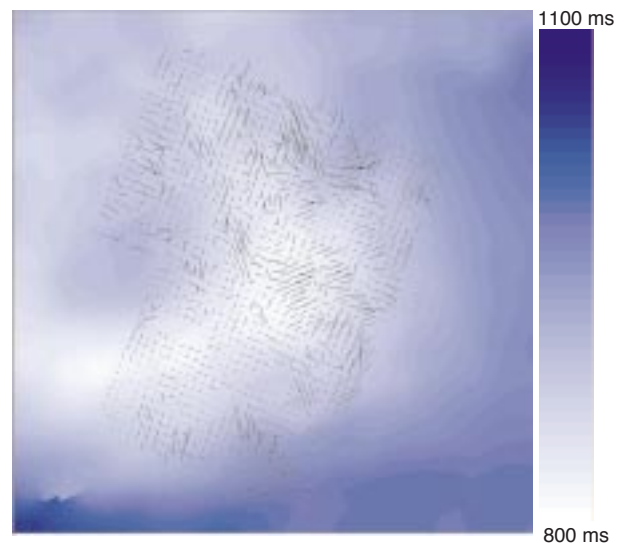


Figure 7  
 $\phi_0$  weighted by  $B$  on top of the picked underlying time horizon.

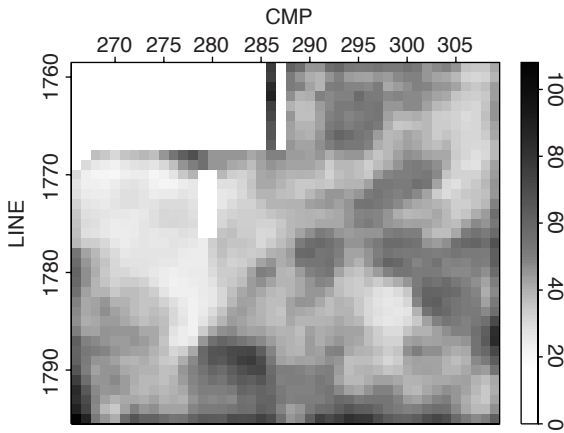


Figure 8  
Standard deviation of  $G$ .

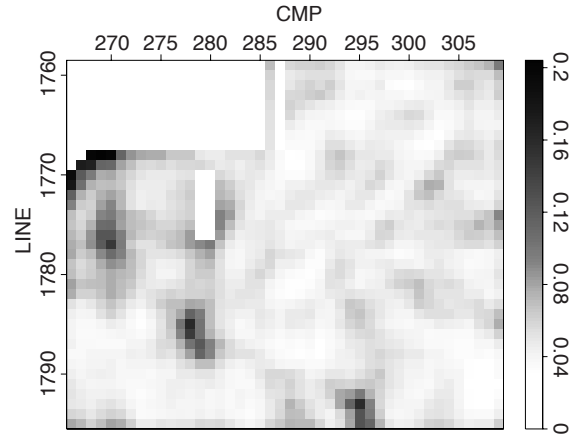


Figure 11  
Normalised standard deviation of  $G$ .

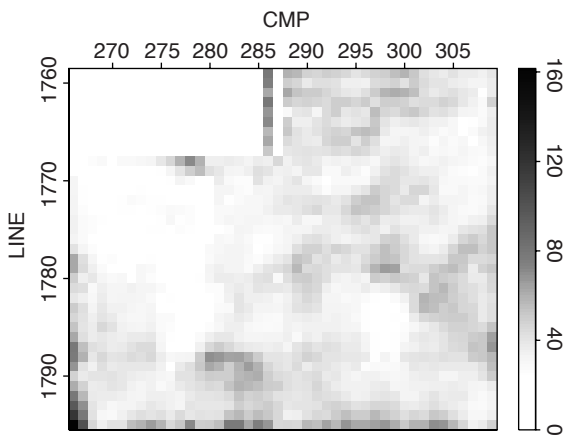


Figure 9  
Standard deviation of  $B$ .

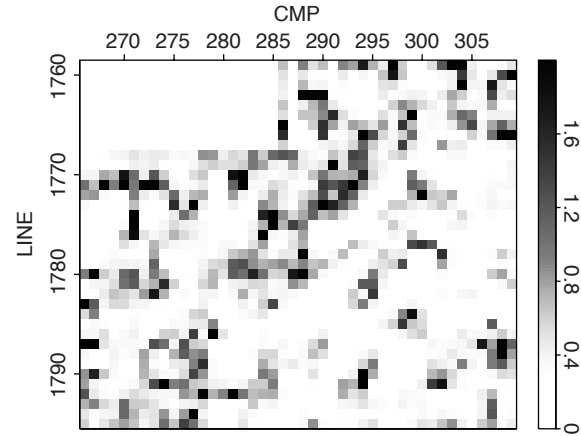


Figure 12  
Normalised standard deviation of  $B$ .

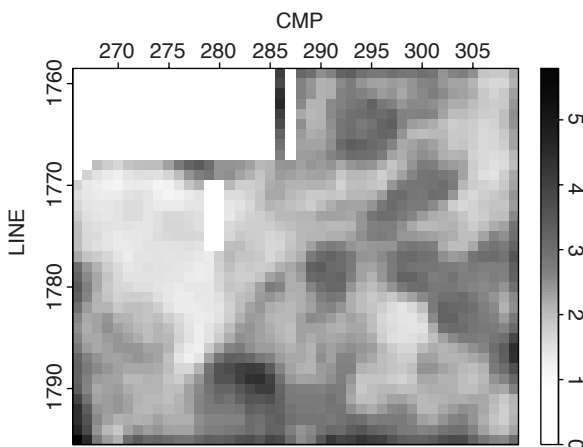


Figure 10  
Standard deviation of  $\phi_0$ .

inferred to be significant. Elsewhere, where the standard deviation of  $B$  is greater than the estimate of  $B$  itself, it is risky to place reliance on the existence of any azimuthal anisotropy.

## DISCUSSION/CONCLUSIONS

We have demonstrated two methodologies for AVOA analysis of 3-D multi-azimuthal seismic datasets on a 1 km x 1 km portion of such data. The first method allows a quick examination of the data for possible trends; the second accounts for variation over offsets, so is a true AVOA inversion, and also allows a quantification of the uncertainties on the estimated parameters. The results from the two methods appear to agree with each other fairly well. The uncertainty

analysis allows us to interpret the results with greater confidence; in particular, we advocate its use in helping decide where the inverted azimuthal variations are significant.

Referring back to Figures 6 and 7, we can see that there is no global trend to the data, as might be caused by a regional stress regime. The underlying horizon in Figure 7 indicates the presence of salt diapirism below, which could be a cause of fracturing above. Around the crest of the dome (line 1783, CMP 286 on Figure 1) there is a possibility of radial fractures to the north, east and south. The strength of these trends could be an indication of the degree of alignment of fractures, their density and/or aspect ratio. The other strong trends near the top of the figures (line 1780, CMP 305) are less easy to assign to the geology, although they do follow closely the contours of the underlying horizon. We are reluctant to attempt further interpretation, which could only be speculative, without any corroborative information from, for example, well data.

## REFERENCES

- Corrigan D. (1990) The effect of azimuthal anisotropy on the variation of reflectivity with offset. Presented at the 4th IWSA.
- Crampin S. (1984) Effective anisotropic elastic constants for wave propagation through cracked solids. *Geophys. J. R. Astr. Soc.*, 76, 135-145.
- Lynn H.B., Simon K.M., Bates C.R., Layman M., Schneider R. and Jones M. (1995) Seismic characterization of a naturally fractured gas reservoir. *65th Annual Internat. Mtg., Soc. Expl. Geophysics*, Expanded Abstracts, 293-296.
- Mallick S., Craft K.L., Meister L.J. and Chambers R.E. (1996) Computation of the principal directions of azimuthal anisotropy from P-wave seismic data. *66th Annual Internat. Mtg., Soc. Expl. Geophysics*, Expanded Abstracts, 1862-1865.
- Rüger A. (1996) Variation of P-wave reflectivity with offset and azimuth in anisotropic media. *66th Annual Internat. Mtg., Soc. Expl. Geophysics*, Expanded Abstracts, 1810-1813.
- Shuey R.T. (1985) A simplification of the Zoeppritz-equations. *Geophysics*, 50, 609-614.
- Thomsen L. (1995) Elastic anisotropy due to aligned cracks in porous rock. *Geophysical Prospecting*, 43, 805-829.

*Final manuscript received in July 1998*